

Article

## The Application of Dielectric Spectroscopy and Biocalorimetry for the Monitoring of Biomass in Immobilized Mammalian Cell Cultures

Harriet E. Cole, Aurélie Demont and Ian W. Marison \*

School of Biotechnology, Dublin City University, Glasnevin, Dublin 9, Ireland;  
E-Mails: harriet.cole2@mail.dcu.ie (H.E.C.); aurelie.demont2@mail.dcu.ie (A.D.)

\* Author to whom correspondence should be addressed; E-Mail: ian.marison@dcu.ie;  
Tel.: +353-1-700-8393.

Academic Editor: Michael Henson

Received: 30 December 2014 / Accepted: 29 April 2015 / Published: 7 May 2015

---

**Abstract:** The purpose of this study was to introduce dielectric spectroscopy and biocalorimetry as monitoring methods to follow immobilised Chinese Hamster Ovary (CHO) cell culture development. The theory behind both monitoring techniques is explained and perfusion cultures are performed in a Reaction Calorimeter (eRC1 from Mettler Toledo) as an application example. The findings of this work show that dielectric spectroscopy gives highly reliable information upon the viable cell density throughout the entire culture. On the other hand, the RC1 could only provide accurate data from day 5, when the cell density exceeded  $4 \times 10^6$  viable cells·mL<sup>-1</sup> (viable cell per mL) working volume (WV). The method validation showed the limit of detection (LOD) for 1.4 L cultures to be  $8.86 \times 10^6$  viable cells·mL<sup>-1</sup>, a viable cell density commonly achieved in fed-batch and the early stages of a perfusion culture. This work suggests that biocalorimetry should be possible to implement at industrial scale to monitor CHO cell cultures.

**Keywords:** mammalian cells; bioprocess monitoring; immobilized cells; dielectric spectroscopy; biocalorimetry

---

## 1. Introduction

Mammalian cells are commonly used to produce biopharmaceuticals as they are capable of correct glycosylation and other post-translational modifications of therapeutic proteins [1–4]. Though continuous cell lines such as Chinese Hamster Ovary (CHO) cells, adapted to suspension culture, are usually encountered in manufacturing processes, it is sometimes more advantageous to use immobilized systems [2]. Cell immobilization not only offers a structure for the cells to grow upon and improve productivity, it also facilitates cell retention in perfusion culture systems.

Perfusion cultures involve continuously supplying the culture with fresh culture media whilst continuously removing the spent media at an identical rate, ensuring the working volume remains constant. This culture type has the advantage to obtain high cell densities whilst continuously supplying the cells with all the essential nutrients and removing all the waste by-products. The cells are usually retained within the reactor by a cell separating device such as a spin filter, cross flow filter, hydrocyclone or acoustic cell settler, Figure 1A. However, these cell separators represent an added cost, can gradually foul or are difficult to scale-up. On the other hand immobilized cultures do not require sophisticated equipment to retain the cells within the vessel. A simple mesh is sufficient to extract the spent media as represented in Figure 1B [5].

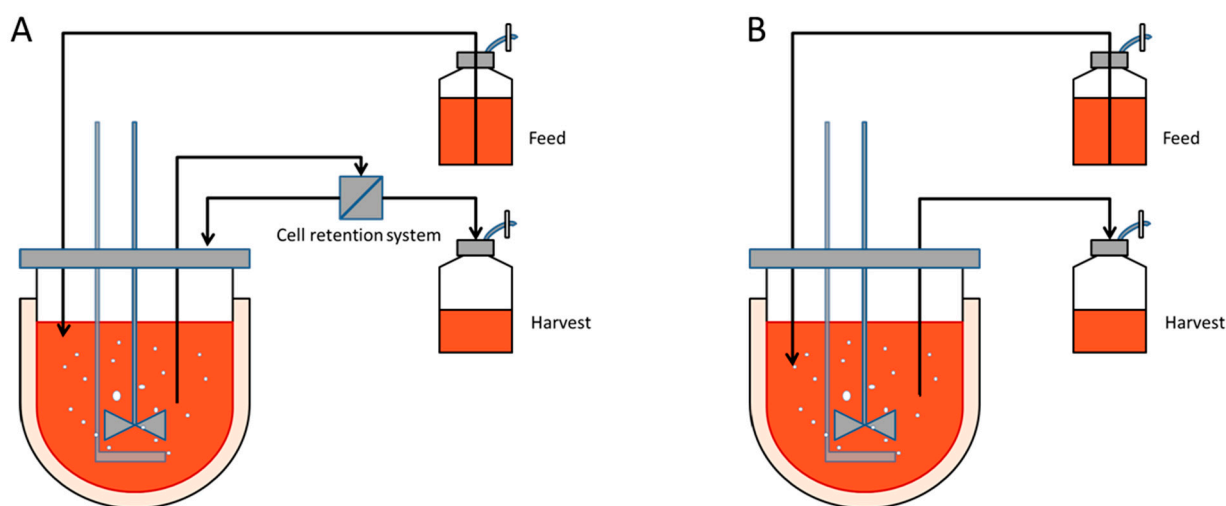


**Figure 1.** Diagram of a perfusion culture setup. (A) Schematic representation of a perfusion culture for suspension cells in a stirred tank reactor. A cell retention system, such as a microfilter, is necessary to separate the cells from spent media; (B) Schematic representation of a perfusion culture for immobilized cells. The microcarriers or microcapsules, typically with a 240  $\mu\text{m}$  radius, are sufficiently large to be retained within the vessel by a wire mesh.

Mammalian cell cultures are highly complex and may vary from one culture to another. To fully characterize a culture each process parameter must be continuously monitored. Biomass quantification and viability determination is a key aspect to any upstream bioprocess. Though cell immobilization offers many advantages, the cells are not readily accessible for culture analysis. Continuously removing a small sample of carriers or microcapsules would mean reducing the available space for the cells to colonize, thus reducing the total number of cells and diminishing the global productivity.

In addition, industrial bioprocesses are moving towards applying different process analytical technologies (PAT) to monitor, and potentially control processes. Since the FDA published the “Guidance for Industry PAT—A Framework for Innovative Pharmaceutical Development, Manufacturing, and Quality Assurance” initiative for Pharmaceutical cGMPs in September 2004, Process Analytical Tools have evolved dramatically [6]. The FDA suggests that the adoption of PAT would help gain a better understanding of the process, which could therefore be better controlled.

These technologies analyse the chemical or physical proprieties of fluids or gases and should be used to improve the process design, development and control. The most commonly used sensors are pH, temperature and DO (dissolved oxygen) probes. However, they can only give limited information and control over complex systems such as cell. Many techniques exist which can potentially measure a wide range of different characteristics from biomass to metabolites and gases [6].

This work seeks to fully colonise microcapsules using a perfusion feed, whilst monitoring the cell physiology using dielectric spectroscopy combined with monitoring the cell metabolic activity using calorimetry. First, based on the known growth kinetics, and microcapsule and cell measurements, the culture time and maximum viable cell density is predicted. The predicted cell density evolution can then be computed into both capacitance and heat flow rates. Subsequently, a feasibility study, to employ an eRC1 (Mettler Toledo, Greifensee, Zürich, Switzerland), a bench-scale calorimeter to follow the cell metabolic activity was undertaken. After validating the monitoring method, a perfusion culture was undertaken in the eRC1 biocalorimetry.

It is the first time, to our knowledge, that CHO cell cultures have been monitored in a bench-scale calorimeter in combination with dielectric spectroscopy. Though this work was only done at bench scale, it also shows the monitoring method potential to be used at larger scale, such as in industrial production processes.

## 2. Biomass Monitoring Methods

Accurate biomass monitoring and control is essential to achieve robust bioprocesses and heterologous protein production. Direct and indirect techniques exist to monitor cell growth and viability. Direct methods measure a physical propriety of a cell and its components, whereas indirect methods measure factors related to the cells and their activity (respiration, electrochemical behaviour, and/or nutrient fluctuation) [7,8].

These technologies should not only have a linear dependence, but be robust, accurate, precise, and easy to calibrate, they must also have no biological interference and endure pressure and temperature conditions of a sterilization process [9]. All of the methods mentioned in Table 1 have certain advantages, but some are not suitable for monitoring encapsulated or other immobilized cell growth and viability. Indeed some methods such as turbidity or multi-wavelength fluorescence would require liberation of the cells from their protective shells or microcarriers. Direct methods are of course preferred as they do not rely on model-based predictions [20], making dielectric spectroscopy a preferred method for monitoring cell encapsulation. This technique relies on the flow of ions, which can easily permeate the microcapsules membrane, in the case of microencapsulated cultures.

An insight into the cell metabolic activity may also offer a better understanding of the bioprocess. Since CO<sub>2</sub> is usually used to control the mammalian cell culture pH, monitoring the carbon dioxide

evolution rate (CER), is not an applicable technique. Nevertheless, biocalorimetry, or the online or at-line monitoring of bioreaction heat generation, may prove to be an easy but informative online monitoring method.

**Table 1.** On-line direct and indirect methods for biomass estimation and applicability to immobilized cell cultures.

PAT	Measured Bioprocess Variable	Direct/Indirect	Applicability to Immobilized Cell Cultures
<b>Dielectric spectroscopy</b>	Capacitance	Direct	Yes
<b>Optical probing</b>	Turbidimetry or nephelometry in VIS or NIR, MIR and FTIR	Direct	No
<b>Multi-wavelength Fluorescence</b>	Cellular fluorophores (NAD(P)H, flavins and aromatic amino acids)	Indirect	No
<b>Biocalorimetry</b>	Heat production from metabolic activity	Indirect	Yes
<b>Off-gas analysis</b>	Oxygen Uptake Rate (OUR) and Carbon Dioxide Evolution Rate (CER)	Indirect	Yes
<b>Infrared sensors</b>	Metabolite concentrations	Indirect	Yes

### 3. Dielectric Spectroscopy

#### 3.1. Cell Suspension as an RC-Circuit?

Cells behave like resistor-capacitor circuits (RC-circuit) when an electrical field is applied to a cell suspension [10,11]. An RC-circuit contains a resistor and a capacitor in series, Figure 2.

A resistor is an energy loss component that transforms electrical energy into heat. A capacitor is an electrical component built with two metal plates separated by a dielectric material, capable of storing electrical charge. A dielectric material, by definition, is an insulating matter containing dipoles which polarise under an electrical field (Figure 3). As suggested by Equation (1) the ability of a capacitor to store charge (capacitance) is dependent on permittivity (ability to transmit an electrical field) and geometry; where  $\epsilon$  is the dielectric permittivity,  $A$  the surface area of the plates,  $d$  the distance between the plates and  $C$  the capacitance.

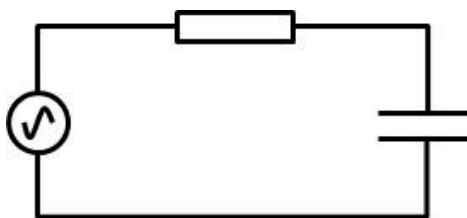


**Figure 2.** Electric diagram of a resistor capacitor circuit.

$$C = \frac{\epsilon \cdot A}{d} \quad (1)$$

When a direct current (DC) passes through a capacitor, the electrical component will polarize and store charge up to its maximum capacity, Figure 3. As soon as the capacitor is fully charged, electrical current can no longer flow through the electrical component. As soon as the fully charged capacitor is connected to another parallel circuit, it will lose the charge and return to its native state.

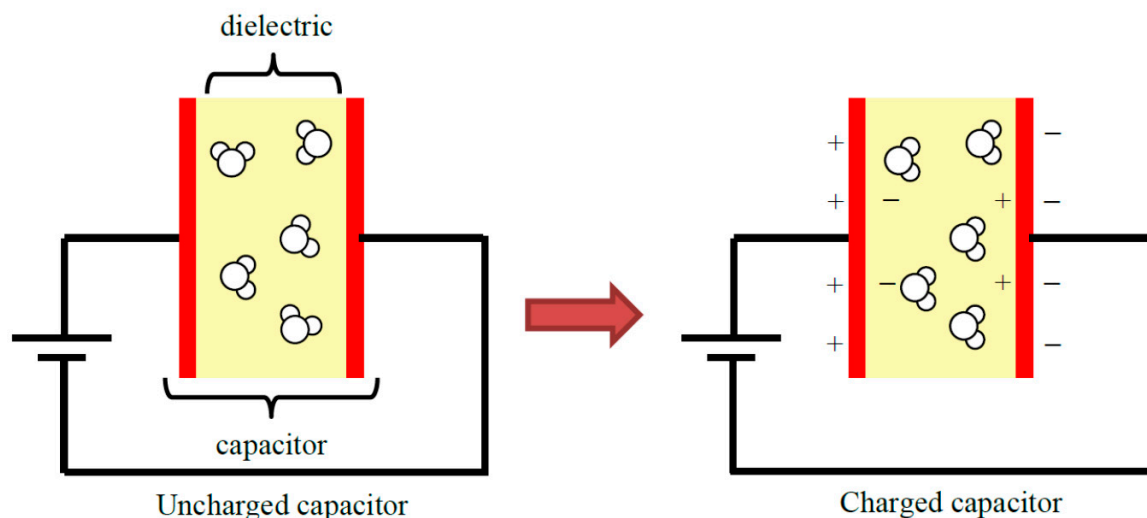


**Figure 3.** Polarization of the dielectric when under an electrical field.

When an alternating current (AC) electrical field flows through a resistor-capacitor field, an amplitude reduction (caused by the resistor) and a phase lag (caused by the capacitor) can be observed between the induced and the response electrical field, Figure 4. An AC field is preferred to other types of alternating current (such as step function current) for the circuit can easily be characterized through a few simple equations. If the input voltage, the resistance and the frequency is known, the amplitude reduction and the phase lag can be determined using the following sequence of equations:

First, the current flowing through the RC circuit (or of a cell suspension) is determined using Ohm and Kirchhoff laws, Equation (2) and Equation (3), with  $U$  being the potential amplitude ( $U_p$  of resistor,  $U_c$  of capacitor, and  $U_e$  of the generator),  $R$  the resistance,  $I$  the current,  $\omega$  the angular frequency,  $C$  the capacitance and  $j$  an imaginary unit.

$$U = R \cdot I \tag{2}$$

$$U_e = U_p + U_c = R \cdot I + I \frac{1}{j \cdot \omega \cdot C} \rightarrow I = \frac{U_e}{R + \frac{1}{j \cdot \omega \cdot C}} = \frac{U_e \cdot j \cdot \omega \cdot C}{j \cdot \omega \cdot C + 1} \tag{3}$$

Then the amplitude or module  $|U_c|$  emitted by the capacitor can be determined using Equation (4).

$$|U_c| = \sqrt{\left(\frac{1}{1 + \omega^2 \cdot R^2 \cdot C^2}\right)^2 + \left(\frac{\omega \cdot R \cdot C}{1 + \omega^2 \cdot R^2 \cdot C^2}\right)^2} \cdot U_e \tag{4}$$

The time shift can also be calculated by determining the argument  $arg|U_c|$  in Equation (5).

$$arg|U_c| = \arctan\left(\frac{-\omega \cdot R \cdot C}{1}\right) \tag{5}$$

This series of equations allows the construction of an oscilloscope diagram, Figure 4, simulating a simple resistor-capacitor circuit constructed in series with an input voltage of 2 Volts alternating at a frequency of 500 kHz, a 2  $\Omega$  resistor and a 412 pF·cm<sup>-1</sup> capacitor.

When an alternating field is applied through a cell suspension, as is the case with a RC-circuit, the cell suspension responds by generating an electrical field with a smaller amplitude but at the same frequency as the input field and with a time shift. Cells may be considered to be microcapacitors since

they can polarize and store charge as they are constructed with a non-conductive phospholipid membrane enclosing a conductive cytoplasm.

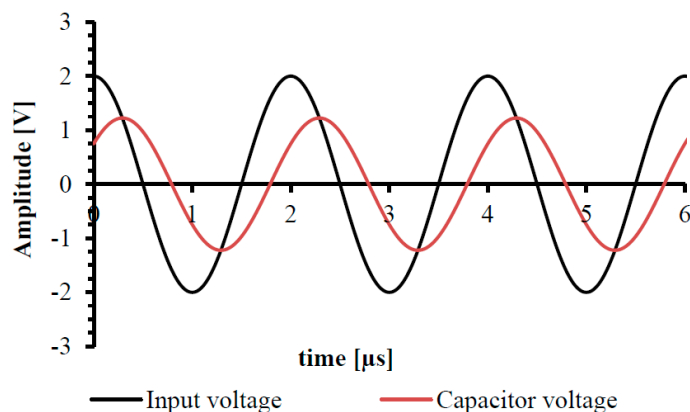


**Figure 4.** The response electrical field amplitude is smaller and shifted from the emitted field. The simulated RC-circuit is built with a 2  $\Omega$  resistor, a 412 pF/cm capacitor. The generator voltage is set at 2 Volts alternating at a frequency of 500 kHz.

In the case of an RC circuit, the component characteristics are known and the amplitude difference and the phase shift can be determined. However dielectric spectroscopy functions conversely. The apparatus generates an alternative electric field at a standard voltage and set frequency. The field polarises the cells, which in turn produce their own electrical field. This field is then measured by the probe electrodes [11]. The apparatus then measures the amplitude difference between the input and response electrical fields and the phase shift. From these measurements, the cell suspension capacitance and conductivity are determined.

### 3.2. Cell Suspension Characterization

As mentioned in Section 3.1, cells can store charge and can be considered to be microcapacitors. Electrically speaking, a healthy cell suspension would consist of three separate electrical regions [12,13]:

- Cell culture medium, a conductive solution containing nutrients and fermentation by-products.
- Plasma membrane which is essentially electrically insulating.
- Cytoplasm, a highly complex but structured combination of water, salts, protein, glycans, nucleic acids and, in eukaryote cells, organelles. Organelles being membrane bound cell sub-structures have an influence on the dielectric response.

When alternating electrical fields are applied to a cell suspension, the ions of the cell culture medium and of the cytoplasm are forced to migrate towards the oppositely charged electrode [14]. The ions within the cytoplasm will be entrapped by the intact plasma membrane, hence polarizing the cell. Solid particles and cells with disrupted plasma membrane (dead cells) do not polarize and will not store charge, Figure 5. However, it is important to note that solid particles, if in a high enough fraction volume could reduce the measured capacitance due to a displacement of the cell containing solution [15].

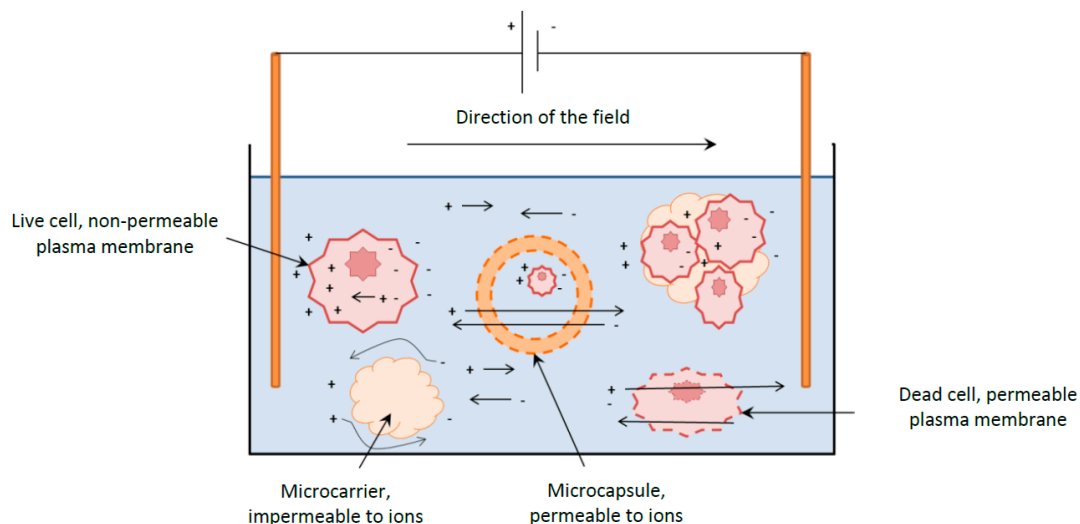


**Figure 5.** Schematic representation showing charge migration within a cell suspension when an electrical current is applied. The positive charge migrates towards the negative electrode and the negative charge towards the positive electrode. Unlike cell debris and solid particles, intact cells entrap ions which consequently polarize them.

The Biomass Monitor from Aber Instruments offers two methods to measure the dielectric characteristics of a cell culture. The first measures continuously the capacitance and the conductivity at a set frequency. The second mode scans and measures the capacitance and the conductivity over 25 pre-set frequencies ranging from  $1 \times 10^5$  Hz to  $1.95 \times 10^7$  Hz [14]. The first mode is easier to implement for cell or microbial culture monitoring and data acquisition, as the displayed information is straight forward and is linearly correlated to the viable biovolume per volume unit of cell suspension. Nevertheless, the second mode, though more complex, gives more comprehensive information about the cell culture, for the ability to polarize a cell at defined electrical frequency is dependent on the cell size, Figure 6 [14–17].

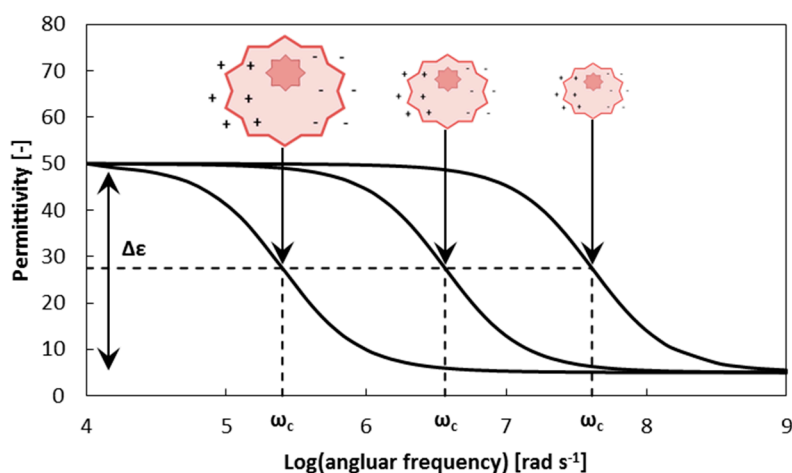


**Figure 6.** The polarisation of a cell at a given electrical frequency is dependent on cell size.

When the electrical field frequency is low, the ions have a sufficient amount of time to flow across the cytoplasm, reach the cell plasma membrane and polarise the cells before the electrical field is

reversed. As the frequency increases, the number of cells that polarise diminishes. The capacitance (or permittivity) measurements are then plotted against the angular frequency in a semi logarithmic plot as represented in Figure 6. The chart therefore displays a  $\beta$ -dispersion, that is characterized by  $\Delta\epsilon$ , the characteristic frequency  $\omega_c$  and  $\alpha$  the slope of the  $\beta$ -dispersion, at  $x = \omega_c$ , Figure 6.  $\Delta\epsilon$  is the permittivity difference between the high and low permittivity plateau and is linearly proportional to the viable cell density (if cell size remains constant), and the characteristic angular frequency  $\omega_c$  is the frequency at which the measured permittivity is equal to  $\Delta\epsilon/2$ . The characteristic angular frequency  $\omega_c$  depends on the cell size. Indeed, ions require more time to reach the plasma membrane before the electrical field is reversed, Figure 6 and Figure 7 [10,11].

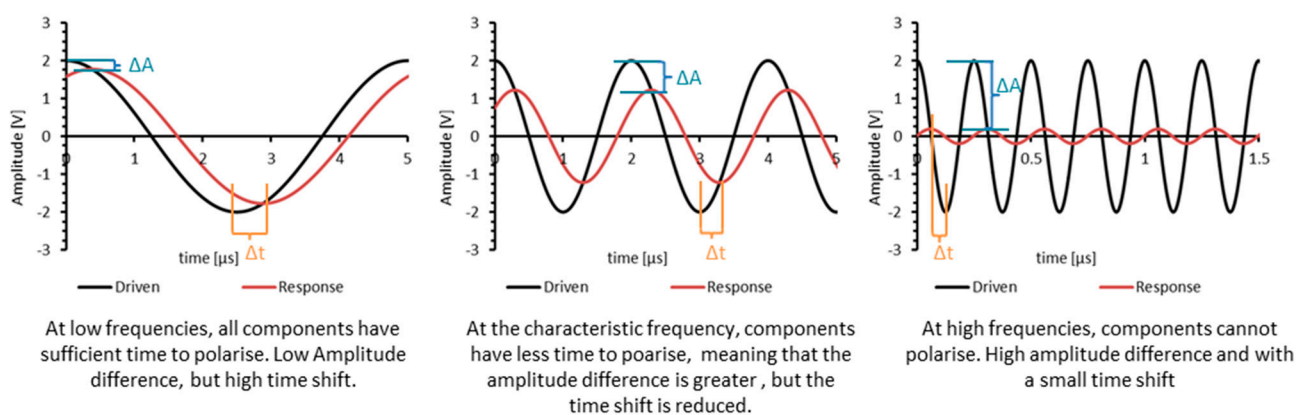


**Figure 7.** At low frequencies, the cells have a sufficient amount of time to polarise, therefore, the time shift is significant and the amplitude difference  $\Delta A$  between the driven and response field is small. At the characteristic frequency  $\omega_c$ , the amplitude difference is greater and the time lag smaller  $\Delta t$ , and at high frequencies no cells polarise, so little signal is measured.

### 3.3. Successful Applications

To obtain a dielectric signal using the biomass monitor of a suspension, a conducting culture medium, an intact insulating cytoplasmic membrane and a conducting cytoplasm is required. At low volume fractions non-biological solid particles or dead cells, with permeable membrane, do not interfere with the dielectric signal [18]. It has been successfully shown that suspension cultures can be monitored on-line using single frequency measurements [19,20] or frequency scans [16,17] in stirred tank reactors.

Immobilized cell cultures may vary slightly from suspension cultures as solid particles are encountered at high volume fractions and may affect the signal [13,18,21]. Because the microcarrier or microcapsule volume fraction should remain constant, a simple calibration of the capacitance *versus* the cell density in the presence of the desired volume fraction of microcarriers is necessary [22]. However, attention must be drawn to microcarrier cultures, as the relationship between capacitance and cell number is only linear until the microcarrier is fully colonised. Once the cells have adhered to the entire available surface, it has been suggested that the cells change not only in size but in shape, affecting the signal [21,22].

Immobilised cell cultures can be undertaken in different types of reactors. Vero cells have been cultivated in a stirred tank perfusion reactor, and successfully monitored using dielectric spectroscopy. The microcarriers were retained using a “home-made” settling glass tube [22]. Different calibration

curves have been established using different microcarrier densities ranging from 1.5 to 6 g·L<sup>-1</sup>. No variations were reported.

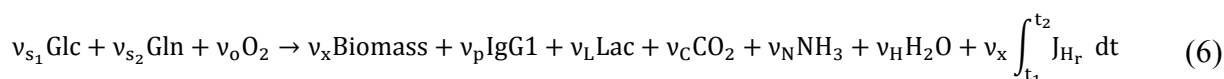
In contrast to stirred tank reactors, immobilised cells can also be cultured in fluidised or packed-bed reactors [15,21]. Sampling in such packed-bed reactors for cell number determination is only possible before inoculation and at the end of the culture. Cell number determination using off-line methods is not possible, meaning a monitoring method is primordial in such cases [21]. On-line capacitance gives real-time information about the culture evolution in both fluidised and packed-bed reactors.

## 4. Biocalorimetry

### 4.1. Cellular Metabolism

Heat production is an inevitable by-product of mammalian cell metabolic activity. [23,24]. Though cells have a tendency to be highly efficient with regards to their energy source, some energy is unavoidably lost in the form of heat. The heat resulting from the cell metabolic activity can be stoichiometrically determined [25].

Mammalian cells have a complex metabolism involving multiple substrates for carbon and energy (they are auxotrophic) and therefore rely on many metabolic pathways. However, a simplified model has been proposed. The stoichiometric equation, assumes that the CHO cells develop solely by metabolising glucose and glutamine as substrates and produce lactate, ammonia and recombinant protein Equation (6) (*Glc*, glucose; *Gln*, L-glutamine; *Lac*, lactate;  $J_{H_r}$ , heat of reaction [23].



### 4.2. Calorimeters

The heat loss can be used to advantage for process monitoring. It has been reported that heat flow is highly correlated to the process biomass [23,26–28]. Microcalorimeters were the first available calorimeters to measure the heat produced by mammalian cells [23,27]. With a high sensitivity they offer the possibility to monitor weak exothermic cultures such as mammalian cell cultures [29]. The microcalorimeters are externally connected to the reactor [23] and continuous samples flow to the calorimetric chamber. The capacity of the calorimetric chamber ranges from (1–100 mL).

Although this heat measuring method is highly sensitive and has shown promising results in measuring the metabolic activity of CHO suspension cultures [23,27], the different environments between the reactor vessel and heat measuring cell can be a major drawback [29,30]. A slight change in pH, aeration, foaming or mixing can affect the cells and their metabolic activity. In addition, the technology can be difficult or impossible to apply to immobilized cell cultures. The removal of microcarriers or microcapsules, if not recycled, would mean a reduction in the total available space for cell colonisation, and hence a diminution in the total cell number and productivity. Finally, this technique is simply not applicable to packed-bed cultures.

Macrocalorimeters generally resemble traditional-bench scale bioreactors, and are much larger with a working volume superior to 1 L [26]. The sensitivity of such calorimeters can vary, especially with the working volume. At small scale, heat production is difficult to measure as most of the heat is lost to the

environment. This heat loss is explained by the high surface to volume ratio of the reactor [29,31]. However, at industrial scale, or at volumes of a few cubic meters, the surface to volume ratio is less significant, and may necessitate cooling instead [32,33].

Different bench- scale calorimeters have been designed and examined. To monitor the heat flux of a mammalian cell culture, high resolution is required. The eRC1-biocalorimeter is the most commonly used macrocalorimeter as it offers a high resolution that is comparable to microcalorimeters ( $15 \text{ mW}\cdot\text{L}^{-1}\cdot\text{K}^{-1}$ ) [26,30].

The RC1 (Mettler Toledo, Greifensee, Zürich, Switzerland) was first designed to characterise the thermodynamics of chemical reactions and has been modified to perform and measure biological reactions (Bio-RC1). Unlike the at-line calorimetric system [23], the Bio-RC1, does not require any additional *ex-situ* equipment to measure the heat production of a culture, it measures the heat production in real-time, and can apply an optimized control of the reactor temperature [30].

#### 4.3. Principles of Bench- Scale Calorimetry

To monitor the heat flux produced during a culture the Bio-RC1 is operated in isothermal mode in which the reactor temperature ( $T_r$ ) is set to remain constant. A silicone oil, circulating at a high rate of  $2 \text{ L}\cdot\text{s}^{-1}$  through the reactor jacket, controls  $T_r$  by adapting the temperature of the jacket ( $T_j$ ) accordingly [26].

The reactor temperature  $T_r$  can be influenced by many parameters and the heat flow accumulated within the reactor can be characterised by the following heat balance, Equation (7) [31]:

$$q_{acr} = q_r - q_j + q_s - q_g - q_e - q_f - q_a - q_{CO_2} + q_c - q_{acj} = 0 \quad (7)$$

$q_{acr}$  and  $q_{acj}$  represent the heat flux accumulated within the reactor and the jacket respectively,  $q_r$  the heat flow produced by the biological reaction(s),  $q_j$  the heat flow to the jacket,  $q_s$  the heat induced by stirring,  $q_g$  the heat loss caused by gassing and evaporation,  $q_e$  the heat loss to the environment,  $q_f$  the heat flow caused by addition of a substrate or medium to the culture,  $q_a$  the addition and dissolution of either an acid and/or a base for the maintenance of a constant pH,  $q_{CO_2}$  the heat flow caused by  $CO_2$  evaporation and  $q_c$  the heat emitted by the calibration heater. The heat flow is expressed in W or equivalently in  $\text{J}\cdot\text{s}^{-1}$ .

As the RC1 is operated in isothermal mode, and most heat fluxes are considered to remain constant throughout the culture, the reaction heat  $q_r$  in the RC1 can be determined using Equation (8).  $U_A [\text{W}\cdot\text{K}^{-1}]$  represents the heat transfer coefficient, or global heat transfer coefficient  $U$  expressed in  $[\text{W}\cdot\text{m}^{-2}\cdot\text{K}^{-1}]$  multiplied by the heat transfer area  $A [\text{m}^2]$ .

$$q_r = U_A \cdot (T_r - T_j) \quad (8)$$

#### 4.4. Bench Scale Biocalorimetry Applications

To our knowledge, no investigation of the use of bench- scale biocalorimeters to monitor mammalian cell cultures has been reported to this date. A number of studies have been reported on the monitoring and possible control of microbial cultures using macrocalorimeters. Biocalorimetry has been used in many different applications, including to monitor culture metabolism and control the feed of nutrients and hence the growth rate. By doing so, respiro-fermentative metabolism caused by overflow metabolism in

Crabtree positive organisms could be avoided [34–38]. In addition, a study was performed in the RC1 to determine the existence of endothermic bacterial strains [39]. By cultivating *Methanosarcina barkeri* and using acetate as substrate under obligate anaerobic conditions, it was shown that the bioreaction was endothermic and yielded  $Y_{Q/x} = 145 \text{ kJ}\cdot\text{C}^{-1}\cdot\text{mol}^{-1}$ .

## 5. Materials and Methods

### 5.1. Cell Line and Culture Conditions

CHO-DP12, a Chinese Hamster Ovary cell line was used for all experiments. CHO-DP12 has been adapted to serum-free medium and secretes a recombinant human IgG1. The cells were cultivated in EX-CELL CHO DHFR<sup>-</sup> (SAFC Biosciences, St. Louis, MO, USA) supplemented with 4 mM L-glutamine, 10 mL·L<sup>-1</sup> Gibco penicillin-streptomycin (Life Technologies, Carlsbad, CA, USA). The inocula was prepared in 1 L shake flasks containing 300 mL of culture medium at 100 rpm and 37 °C.

The BioRC1 (Mettler Toledo, Greifensee, Zürich, Switzerland) was inoculated with 25% (v/v) Ca<sup>2+</sup>-alginate-poly-L-lysine-alginate (APLLA) microcapsules containing 1 × 10<sup>6</sup> cells·mL<sup>-1</sup> alginate, equivalent to 300 mL of packed microcapsules containing a total of 3 × 10<sup>8</sup> cells corresponding to an initial cell density of 0.3 × 10<sup>6</sup> vcells·mL<sup>-1</sup>vv (viable cells per mL working volume) in a working volume of 1400 mL medium. The culture conditions were monitored and controlled to a set-point of 37 °C and pH 7.2. The pH was maintained at 7.2 by a continuous CO<sub>2</sub> headspace enrichment initially set at 5%. As the culture pH stabilises and requires less acidification of the suspension, the enrichment was reduced manually, step-wise, and then switched off. The alkali addition to maintain the pH at 7.2, was executed by the pH controller (Bioengineering, Wald, Zürich, Switzerland). It was desired to have punctual base addition, to avoid calorimetric signal interference, consequently the controller was fixed at pH = 7.2 ± 0.2, T<sub>ON</sub>/T<sub>OFF</sub> potentiometers, controlling opening or closing times are set to obtain punctual addition, that would translate to a spike in the signal. Agitation used a pitched- blade disc turbine impeller rotating at 100 rpm. Air was sparged into the culture media at 0.01 vvm and the headspace aerated at 0.1 vvm. The viable cell density was monitored using a Biomass monitor (ABER Instruments, Aberystwyth, Ceredigion, UK), and was set on dual frequency and polarisation correction, at 580 kHz and 10,085 kHz (3.64 × 10<sup>6</sup> (rad·s<sup>-1</sup>) and 6.34 × 10<sup>9</sup> (rad·s<sup>-1</sup>)). The capacitance readings as well as the reactor and jacket temperatures were collected and saved in a text file using an in-house designed LabVIEW program.

After inoculation, the cells were allowed to develop to 2 × 10<sup>6</sup> vcells·mL<sup>-1</sup> in batch mode at which point the perfusion feed was initiated. The feed was set at a dilution rate  $D = 2\cdot\mu_{max}$ , to avoid early nutrient depletion, extracapsular cell wash-out as well as an important accumulation of waste metabolic by-products. This meant that over a 24 h period, 1.7 L of feed was supplied to the culture, and 1.7 L of spent media containing extracapsular cells and microcapsule debris was removed.

The EX-CELL CHO DHFR<sup>-</sup> medium contains approximately 6 g·L<sup>-1</sup> glucose and was supplemented with 4 mM L-glutamine. The total daily glucose and L-glutamine requirements for the following 24 h were calculated on a daily basis using Equation (9), where  $S$  is the substrate,  $q_s$ , the specific substrate uptake rate,  $X$  the total number of viable cells in the culture and  $\mu$  the growth rate and  $t$  time. If necessary, the feed was supplemented with additional glucose and L-glutamine.

$$S = q_s \cdot (X \cdot e^{\mu \cdot t}) \cdot t \quad (9)$$

### 5.2. Cell Microencapsulation

The microcapsules were produced by extruding a cell suspension in 1.5% alginate solution through an Encapsulator Biotech (Inotech, Basel, Switzerland). Cells ( $3.4 \times 10^8$ ) were centrifuged at  $200 \times g$  for 10 min and re-suspended in 340 mL of sterile filtered 1.5% (w/v) sodium alginate, 10 mM MOPS (Sigma Aldrich, St. Louis, MO, USA; Cat#: M3183) and 0.85% NaCl (Merck, Darmstadt, Hesse, Germany; Cat#: 106400) buffer, pH 7.2. The alginate-cell suspension was then extruded through a 200  $\mu\text{m}$  diameter single nozzle into a stirred 1 L solution of 100 mM  $\text{CaCl}_2$  (Sigma, St. Louis, MO, USA; Cat#: C7902) in 10 mM MOPS buffer pH 7.2. After incubation for 10 min, the  $\text{CaCl}_2$  solution was removed and the alginate beads washed with 500 mL 10 mM MOPS containing 0.85% NaCl. After washing, the  $\text{Ca}^{2+}$ -alginate beads were placed in a 0.05% (w/v) solution of 30,000–70,000 Dalton poly-L-lysine hydrobromide (Sigma Aldrich, St. Louis, MO, USA; Cat#: P2636) in 10 mM MOPS, 100 mM  $\text{CaCl}_2$ , pH 7.2 for 30 min. After coating with PLL the beads were washed twice for five minutes with the MOPS-NaCl buffer pH 7.2, and coated with a second layer of Na-alginate by incubation in a 0.03% (w/v) sodium alginate, 10 mM MOPS, 0.85% NaCl, pH 7.2 for 10 min. The coated beads were once again washed twice with MOPS-NaCl buffer and the inner  $\text{Ca}^{2+}$ -alginate core solubilised by addition of a 1 L solution containing 50 mM sodium citrate (Sigma Aldrich, St. Louis, MO, USA; Cat#: S1804), 10 mM MOPS, 0.85% NaCl, pH 7.4. The APLLA microcapsules were washed once with 500 mL MOPS-NaCl buffer, and once with 300 mL non-supplemented media. After removing the medium, 300 mL of supplemented medium was added to the microcapsules. The cell-containing microcapsules were then transferred into an inoculating bottle and aseptically connected to the bioreactor for inoculation.

### 5.3. Microcapsule Break-up Method

To determine the viable cell density off-line, the cells need to be liberated from the microcapsules. The microcapsule break-up method used must be rapid and gentle in order to not affect the cell viability. First, the microcapsules were separated from the medium using a cell strainer (100  $\mu\text{m}$  nylon mesh) and washed with PBS. The microcapsules were then transferred to a graduated 1 mL syringe connected to a 30 gauge needle. A ratio of 1:1 volume PBS to microcapsules was added before extruding the microcapsules through the needle. The broken PBS/microcapsule suspension was extruded twice more to ensure complete microcapsule breakage and to avoid the presence of particles which might interfere with the cell counting. The liberated cells were counted microscopically using a Neubauer Haemocytometer after staining with 0.4% Trypan blue.

### 5.4. Off-Line Measurements

The concentration of glucose and lactate in culture samples was quantified using an HPLC (Agilent Instruments 1200, Agilent Technologies Ltd., Santa Clara, CA, USA) equipped with a refractive index detector, thermostat set to 30 °C with a Supelcogel™ C-610H column (Sigma Aldrich, St. Louis, MO, USA). A 0.01 M  $\text{H}_2\text{SO}_4$  solution was used as mobile phase at a constant rate of  $0.5 \text{ mL} \cdot \text{min}^{-1}$  for 32 min.

L-Glutamine and ammonia concentrations were quantified using commercially available enzyme assay procedures (Megazyme, Bray, Wicklow, Ireland), in which the absorbance was measured using a Versamax microplate reader (Molecular Devices, Sunnyvale, CA, USA).

Recombinant IgG<sub>1</sub> was quantified using protein A affinity HPLC. The HPLC (Agilent Instruments 1200, Agilent Technologies Ltd., Santa Clara, CA, USA) was equipped with a refrigerated autosampler and a thermostatted column compartment. The column, POROS<sup>®</sup> Prepacked Protein A Affinity Column (Life Technologies, Thermo Fisher Scientific, Carlsbad, CA, USA) was connected and maintained at 25 °C. Two mobile phases were prepared: Mobile Phase A—20 mM sodium phosphate, 500 mM NaCl, pH 7.0; Mobile Phase B—50 mM sodium phosphate, 500 mM NaCl, pH 2.0.

Each analysis lasted 5 min. The flow rate of the two mobile phases was 2 mL·min<sup>-1</sup>, and according to the program described in Table 2. Culture samples 25 µL were injected in 100% of mobile phase A. The recombinant protein was detected using a UV/VIS detector set to 280 nm.

**Table 2.** Elution program for the quantification of IgG<sub>1</sub> by affinity HPLC.

Time	% Mobile Phase A	% Mobile Phase B
0.0 → 2.5 min	100	0
2.5 → 3.5 min	0	100
3.5 → 5.0 min	100	0

To ensure column efficiency, the protein column must be regenerated at the beginning and the end of the process, after the calibration curve samples, after every 20 samples and at the end of the sequence. This was done by injecting 3 × 100 µL of 2 M guanidine HCl and eluting using the mobile phase B at 2 mL·min<sup>-1</sup>. The column regeneration was followed by 3 blank analysis, (3 injections of mobile phase A).

## 6. Results

### 6.1. Culture Predictions

The average microcapsule radius was 260 µm. The membrane thickness of the microcapsule, was evaluated to be 18 µm by confocal microscopy, (Figure 8) and thus the average internal volume and potential colonisation space represented 4.71 × 10<sup>7</sup> µm<sup>3</sup>. The cell volume being 115 µm<sup>3</sup>, (radius = 6.5 µm), would entail the microcapsules having a maximum colonisation potential of 6.40 × 10<sup>4</sup> cells·capsule<sup>-1</sup>.

The work involved monitoring microencapsulated cell densities in approximately 25% (v/v) microcapsule cultures. Therefore, a culture, without any inhibitory factors, may generate cell densities up to 139 × 10<sup>6</sup> cells·mL<sup>-1</sup>. Providing the cells grow constantly at 0.62 days<sup>-1</sup>, without a lag phase, the full microcapsule core colonisation should be achieved after 11.3 days. Based on the CHO-DP 12 specific capacitance, 1.44 × 10<sup>-6</sup> pF·mL·cm<sup>-1</sup>·cell<sup>-1</sup>, such densities would have a capacitance reading of 200.1 pF·cm<sup>-1</sup>, as illustrated in Figure 9A. It is expected that once the maximum cell density is achieved, and the metabolites are present in the adequate concentrations, that the capacitance would remain stable [23].

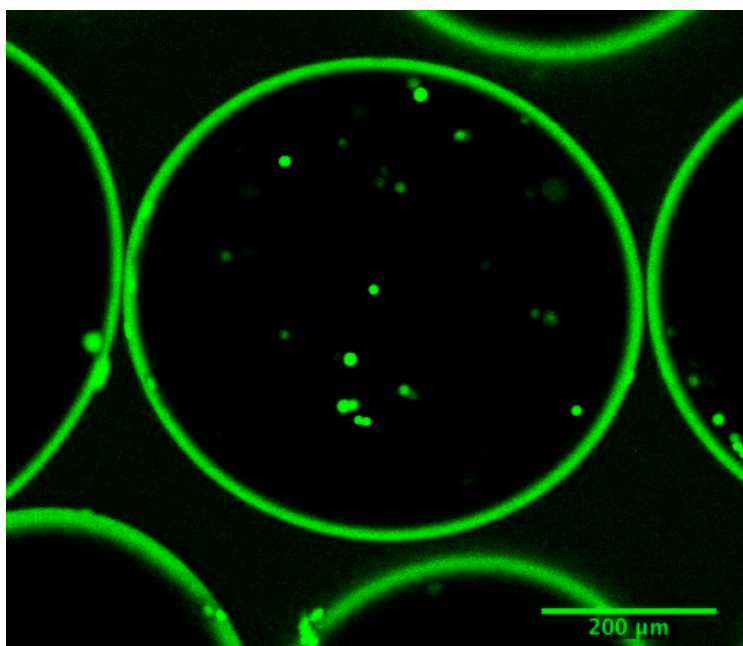


**Figure 8.** Confocal image of calcium-alginate poly-L-lysine-alginate microcapsules, immediately after inoculation. The average microcapsule radius is 260  $\mu\text{m}$  and the membrane thickness, 18  $\mu\text{m}$ . The stained cells fluoresce green if viable, or red if dead.

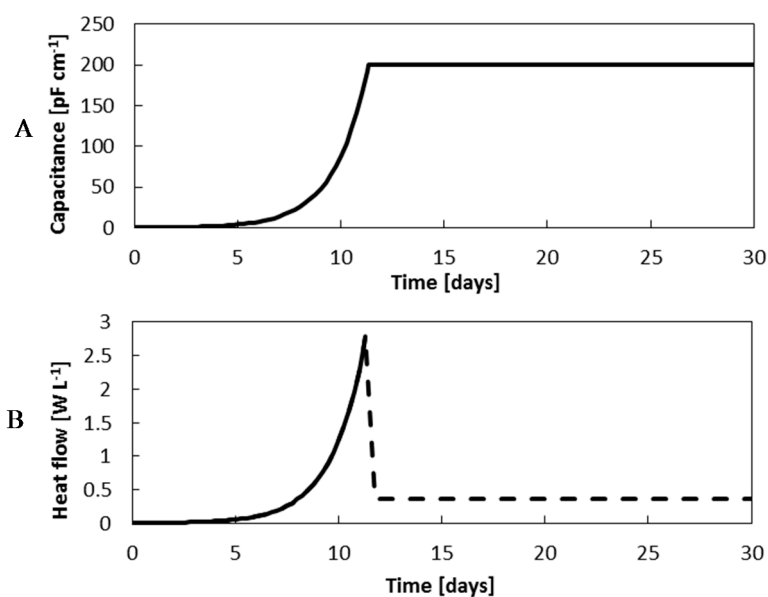


**Figure 9.** Capacitance (A) and heat flow (B) predictions throughout the exponential phase, assuming the cells duplicate at the maximum growth rate  $\mu_{\text{max}} = 0.64 \text{ day}^{-1}$ , and the stationary phase, when the full microcapsule colonisation potential has been achieved.

In addition to the continuous capacitance readings, the heat produced by the cells will be monitored by the eRC1 calorimeter. In the literature, it has been reported that mammalian cells produce very little heat in contrast to microbial cells [30,40]. More specifically, the specific heat flow rate of the CHO 320 cell line was evaluated at its peak at 20 pW cell<sup>-1</sup> [23]. Consequently, it is expected for the heat flow rate to increase at the same rate as the cells and capacitance up to 2.8 W·L<sup>-1</sup>. Once the cells have no longer any free space to replicate, the cell growth should become inhibited. As the heat flow rate is

dependent upon the metabolic rate, it is forecast for the heat signal to fall and stabilise at an inferior heat flow rate, Figure 9B, [36,37].

The eRC1 calorimeter resolution has a reported resolution of to be  $50 \text{ mW}\cdot\text{L}^{-1}$ . This means for a 1.4 L CHO culture, the Limit of blank (LOB), or the maximum cell density that can still be considered as a blank sample, should not exceed  $3.5 \times 10^6 \text{ vcells}\cdot\text{mL}^{-1}\text{wv}$ . The lowest measurable cell density, or the Limit of Detection (LOD) was estimated at approximately  $11.6 \times 10^6 \text{ vcells}\cdot\text{mL}^{-1}\text{wv}$ . Therefore, the calorimetric method is not sufficiently sensitive to monitor batch cell cultures. However, biocalorimetry has a promising potential to monitor the biomass development stage of microencapsulated CHO cell perfusion cultures that are projected to exceed these densities.

### 6.2. Biocalorimetry Monitoring Method Validation for CHO Cell Cultures

The heat signal plotted against the cell density display a linear trend, which was modelled by linear regression. The data points were found to be linearly correlated with a coefficient  $R = 0.99$ . The slope of the linear regression, corresponding to the specific cellular heat flow is estimated at  $74.77 \pm 5.66 \text{ pW}\cdot\text{cell}^{-1}$ , Figure 10.

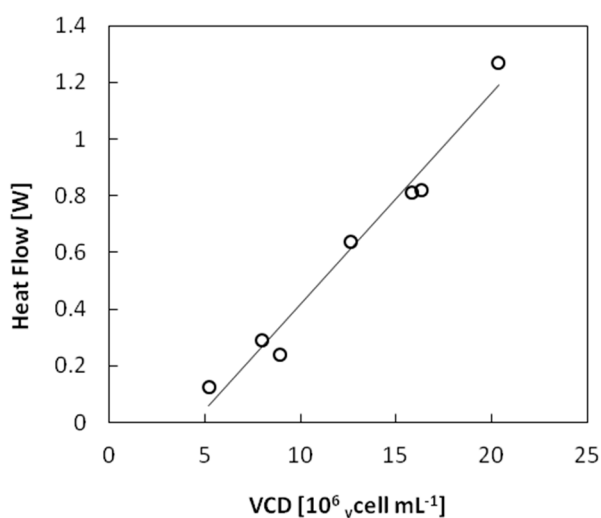


**Figure 10.** Heat flow rate and viable cell density linear model. The linear regression is constructed with a slope  $a = 74.77 \times 10^{-11} \text{ W}\cdot\text{cell}^{-1}$  and a correlation coefficient of  $R = 0.99$ .

From the linear regression analysis, the LOB, LOD and LOQ were established, Table 3. The LOB, LOD and Limit of Quantification (LOQ) were calculated following the ICH Harmonised Tripartite Guideline's "Validation of Analytical Procedures: Text and Methodology Q2(R1)" published in November 2005. From the linear regression, the limit of the blank is evaluated at  $1.33 \times 10^6 \text{ vcells}\cdot\text{mL}^{-1}\text{wv}$  and the lowest possible cell density to be properly detected was evaluated at  $8.87 \times 10^6 \text{ vcells}\cdot\text{mL}^{-1}\text{wv}$ . Cell densities above  $26.88 \times 10^6 \text{ vcells}\cdot\text{mL}^{-1}\text{wv}$ , according to the ICH method, should be reliably quantified.

These findings are comparable to the predicted method limits presented in sub-section 6.1. Both the predicted limit of detection, evaluated at  $11.55 \times 10^6 \text{ vcells}\cdot\text{mL}^{-1}\text{wv}$ , and the one based on the calibration model  $8.87 \times 10^6 \text{ vcells}\cdot\text{mL}^{-1}\text{wv}$  are of the same magnitude. Nevertheless, this confirms the conclusion that bench scale calorimetry using the eRC1 is not a sensitive enough method to monitor 1.4 L CHO-DP12 suspension cultures, but has a strong potential to monitor microencapsulated perfusion

cultures. Microencapsulated cultures, with a 25% (v/v) microcapsules to medium working volume ratio are expected to reach densities above  $10^8$   $\nu\text{cells}\cdot\text{mL}^{-1}_{\text{wv}}$  and according to the specific heat flow rate, should generate heat flows above  $2.5 \text{ W}\cdot\text{L}^{-1}$ .

**Table 3.** Monitoring encapsulated CHO-DP12 cell cultures method validation.

Method Validation Characteristics	Values
Specific cellular heat flow rate	$74.77 \pm 5.66 \text{ pW}\cdot\text{cell}^{-1}$
Standard deviation of the ordinate	0.201 W
Limit of blank	$1.33 \times 10^6 \nu\text{cells}\cdot\text{mL}^{-1}_{\text{wv}}$
Limit of detection	$8.87 \times 10^6 \nu\text{cells}\cdot\text{mL}^{-1}_{\text{wv}}$
Limit of quantification	$26.88 \times 10^6 \nu\text{cells}\cdot\text{mL}^{-1}_{\text{wv}}$

### 6.3. Perfusion Cultures Cell Density and Metabolite Analysis

The perfusion cultures were operated in two distinct phases: batch and perfusion phase. The batch phase lasted 4 days, until the viable cell density reached  $1.7 \times 10^6 \nu\text{cells}\cdot\text{mL}^{-1}_{\text{wv}}$ . The feed was then supplied at  $1.7 \text{ L}\cdot\text{day}^{-1}$  for a duration of 8 days, and ended 12 days after inoculation. A maximum cell density of  $15 \times 10^6 \nu\text{cells}\cdot\text{mL}^{-1}_{\text{wv}}$  was achieved; a 5-fold augmentation of the viable cell density compared to batch cultures ( $3 \times 10^6 \nu\text{cells}\cdot\text{mL}^{-1}_{\text{wv}}$ ). The viability remained above 80% throughout, yet the fall in the viable cell density on day 12 was caused by loss of microcapsule stability. The released cells from the ruptured microcapsules were then washed out with the media outflow.

The viable cell density was estimated using three different methods: offline by counting cells under the microscope, by continuous real-time dielectric measurements and the continuous real-time calorimetry measurements. The continuous capacitance measurements were computed into viable cell number by dividing the capacitance with the CHO-DP 12 specific capacitance,  $1.44 \times 10^{-6} \text{ pF}\cdot\text{mL}\cdot\text{cm}^{-1}\cdot\text{cell}^{-1}$ , and the heat flow rate using the calibration model proposed in Section 6.2. The viable cell density, assessed by the three monitoring methods throughout the full culture time, is displayed in Figure 11.

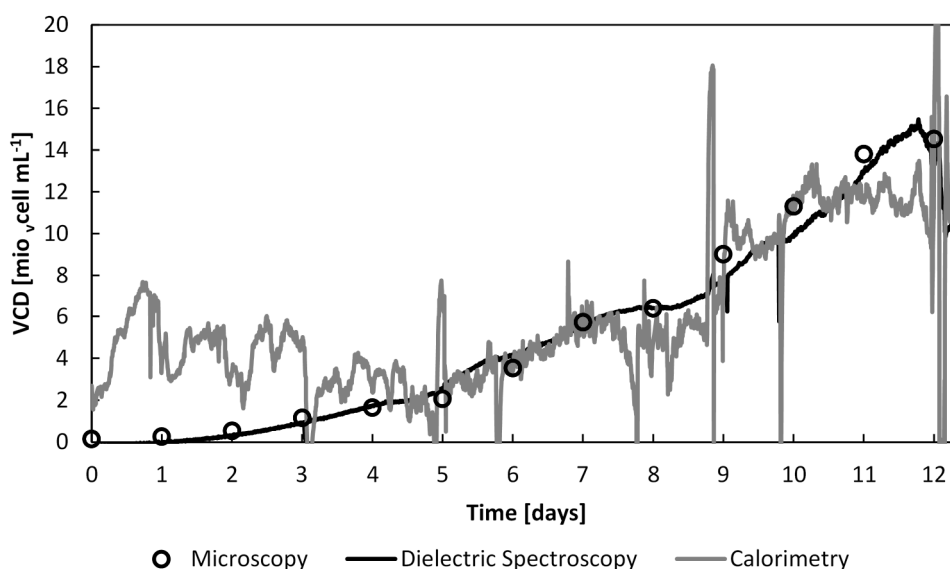


**Figure 11.** The viable cell density evolution throughout the whole culture time estimated by off-line cell counts, dielectric spectroscopy and calorimetry.

As expected, and previously demonstrated, the cell density determined by dielectric spectroscopy and microscopy are highly correlated, from the beginning of the culture. On the other hand, the heat flow rate measurements did not provide accurate information before day 6, after which the cell density was above  $4 \times 10^6$   $\text{vcells}\cdot\text{mL}^{-1}\text{wv}$ .

The headspace of the culture was enriched with initially 5%  $\text{CO}_2$  to stabilise the pH between 7.2 and 7.4. With the progression of the culture and the accumulation of lactate, Figure 12, the  $\text{CO}_2$  enrichment is punctually diminished, once a day, when sampling, to avoid the pH dropping below 7. This was undertaken to avoid unnecessary NaOH addition to the culture and calorimetric signal interference. The step-wise reduction off  $\text{CO}_2$  has subsequently an effect on the heat signal. Indeed, the dissolution of  $\text{CO}_2$  into water has an enthalpy of  $-375 \text{ kJ}\cdot\text{kg}^{-1}$  or  $-16.5 \text{ kJ}\cdot\text{kg}^{-1}$  [41].

Moreover, a shift of metabolism occurred after day 10. The heat flow rate evolved in a similar manner to the offline cell counts and online capacitance data. However, after day 10, the heat flow rate stabilises at 0.8 W, the equivalent of at  $11 \times 10^6$   $\text{vcells}\cdot\text{mL}^{-1}\text{wv}$ . This stabilisation of the heat flow rate signal may be explained by the observed reduction of the microencapsulated cell growth rate by 50% from  $0.62 \text{ day}^{-1}$  to  $0.29 \text{ day}^{-1}$ .

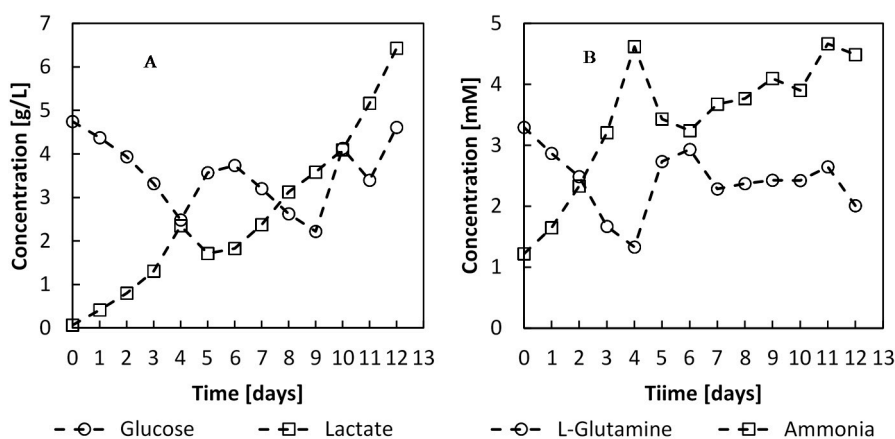


**Figure 12.** Metabolite concentrations during the batch and perfusion phases of the culture. The perfusion phase was initiated on day 4 with a feed rate of  $1.7 \text{ L}\cdot\text{day}^{-1}$ .

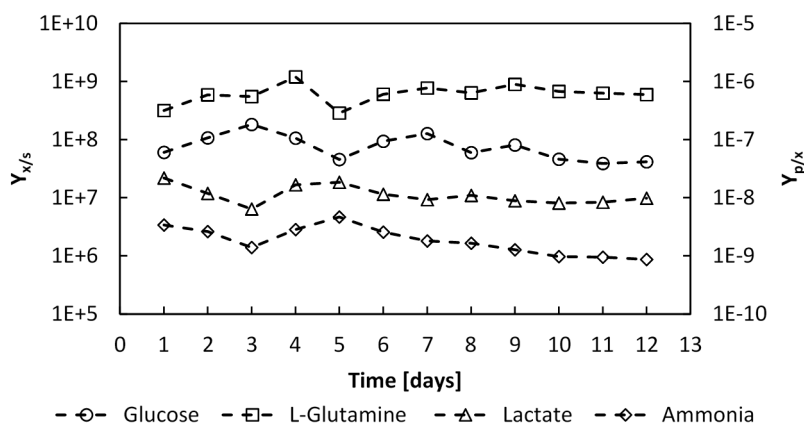


**Figure 13.** Evolution of the glucose and L-glutamine to number of cells yields  $Y_{X/S}$ , and the produced lactate and ammonia to cells yields,  $Y_{P/X}$ , over the whole culture period, expressed in  $(\text{cells}\cdot\text{mmol}^{-1})$  and  $(\text{mmol}\cdot\text{cell}^{-1})$  respectively.

The substrate to biomass yields were determined during the batch phase to be  $Y_{X/glc} = 1.28 \times 10^8 \text{ cells} \cdot \text{mmol}^{-1}$  and  $Y_{X/gln} = 8.66 \times 10^8 \text{ cells} \cdot \text{mmol}^{-1}$ , and remained constant throughout the perfusion phase, Figure 13. The product to biomass yields also remained constant with values of  $Y_{Lac/X} = 1.18 \times 10^{-8} \text{ mmol} \cdot \text{cell}^{-1}$  and  $Y_{NH_3/X} = 2.09 \times 10^{-9} \text{ mmol} \cdot \text{cell}^{-1}$ . Thus, since the substrate to biomass yield and product to biomass yields remained constant throughout the culture, this would indicate that no shift in the catabolic pathways occurred.

The perfusion feed, initiated on day 4, provided the cells with sufficient glucose and L-glutamine for optimal growth, and these nutrients did not become limiting (Figure 12). The perfusion feed and continuous removal of medium reduced the accumulation of metabolic by-products, which may have important undesirable cell growth inhibition effects and change the protein glycosylation profile [42–44]. After day 10, the lactate concentration was found to be up to  $4 \text{ g} \cdot \text{L}^{-1}$ , and accumulated up to  $6.4 \text{ g} \cdot \text{L}^{-1}$ , and the cell growth rate dropped to  $0.29 \text{ day}^{-1}$ .

Finally, the CHO-DP12 cells produced a recombinant IgG<sub>1</sub> protein at the rate of  $25.52 \text{ pg} \cdot \text{cell}^{-1} \cdot \text{day}^{-1}$ . The perfusion culture generated a total of 2.4 g of IgG<sub>1</sub>, Figure 14, which is 39.7-fold the amount synthesised in a batch culture.

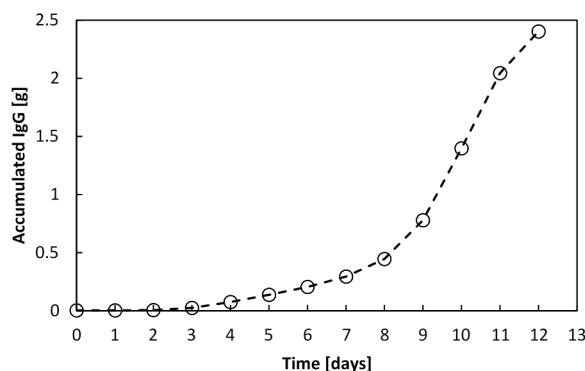


**Figure 14.** Accumulated recombinant IgG<sub>1</sub> manufactured by an encapsulated cell perfusion culture. After 12 days, 2.4 g of IgG<sub>1</sub> was produced by  $14.5 \times 10^6 \text{ vcells} \cdot \text{mL}^{-1} \text{ wv}$  in a 1.4 L culture.

## 7. Conclusions

Mammalian cell cultures are complex processes and can have important batch- to- batch variations therefore, monitoring mammalian cells is critical. Immobilised cell cultures have an additional barrier to real-time monitoring as the cells are not directly available for analysis. Nevertheless, both dielectric spectroscopy and biocalorimetry were shown to have potential at all scales of operation. Dielectric spectroscopy offers direct viable cell number monitoring in different types of immobilized mammalian cell culture. Though a calibration may be necessary, the signal is not influenced by the presence of the microcarriers (or microcapsules). Biocalorimetry is readily applicable at large- scale through simple heat balancing methods, but necessitates more sophisticated equipment at bench- sale. Though no studies have investigated the potential use of laboratory scale calorimeters, the RC1 calorimeter has a resolution comparable to microcalorimeters which have previously been used to monitor CHO suspension cells.

The perfusion culture yielded viable cell density of  $15 \times 10^6 \text{ vcells} \cdot \text{mL}^{-1} \text{ wv}$ , a 5-fold higher density in comparison to batch cultures. The microcapsules contained an average of  $1.34 \times 10^4 \text{ cells} \cdot \text{capsule}^{-1}$ , representing 43.6% of the microcapsule internal volume. The cell development was monitored on-line

by dielectric spectroscopy and biocalorimetry. Both capacitance and heat flow rate measurements correlated with viable cell density using the calibration models and compared to the viable cell density determined off-line microscopically, counted under the microscope. The capacitance signal followed cell growth reliably, from inoculation through to the decline phase. The heat signal also provided accurate information upon the culture development from day 6 onwards, from  $4 \times 10^6$  vcells·mL<sup>-1</sup><sub>wv</sub>. Between day 6 and day 10, the cells grew at a rate of 0.62 day<sup>-1</sup>. Although no apparent change in the analysed substrates and products to biomass yields was observed, after day 10, the growth rate fell to 0.29 day<sup>-1</sup>.

Reaction calorimetry can follow cellular activity of high cell densities but can precisely quantify the number of cells per unit volume only above  $26.88 \times 10^6$  vcells·mL<sup>-1</sup><sub>wv</sub>. Higher cell densities are theoretically achievable, but further microcapsule stabilisation studies must be undertaken to avoid capsule breakage and associated cell loss.

Additionally, this study is a stepping stone towards using continuous heat flow rate measurements to evaluate in real-time cell activity at industrial scale. This work involved growing cells in a working volume of 1.4 L. At this scale, the surface area to volume ratio is high, consequently, the heat losses to the environment are significantly [31,45]. However, large reactors e.g., 12.5 m<sup>3</sup> have a much lower surface area to volume ratio, meaning that the heat loss is much smaller. Therefore, a larger difference between  $T_r$  and  $T_j$  is necessary to maintain the CHO culture at the set reactor temperature, [32,33] and accurate heat flow measurements can be made.

## Acknowledgments

The Science Foundation Ireland is greatly acknowledged for the financial support of this work under grant no. 08/IN.1/B1948.

## Author Contributions

Harriet E. Cole, Aurélie Demont and Ian W. Marison conceived and designed the experiments; Harriet E. Cole and Aurélie Demont performed the experiments; Harriet E. Cole analysed the presented data; Ian W. Marison directed the work and contributed to reagents/materials/analysis tools; Harriet E. Cole and Ian W. Marison wrote the paper.

## Conflicts of Interest

The authors declare no conflict of interest.

## References

1. Ozturk, S.; Hu, W.-S. *Cell Culture Technology for Pharmaceutical and Cell-Based Therapies*; CRC Press: Boca Raton, FL, USA, 2005.
2. Tharmalingam, T.; Sunley, K.; Spearman, M.; Butler, M. Enhanced Production of Human Recombinant Proteins from CHO cells Grown to High Densities in Macroporous Microcarriers. *Mol. Biotechnol.* **2011**, *49*, 263–276.

3. Wurm, F.M. Production of recombinant protein therapeutics in cultivated mammalian cells. *Nat. Biotechnol.* **2004**, *22*, 1393–1398.
4. Zhu, J. Mammalian cell protein expression for biopharmaceutical production. *Biotechnol. Adv.* **2012**, *30*, 1158–1170.
5. Breguet, V.; Gugerli, R.; von Stockar, U.; Marison, I.W. CHO immobilization in alginate/poly-L-lysine microcapsules: An understanding of potential and limitations. *Cytotechnology* **2007**, *53*, 81–93.
6. Bakeev, K.A. *Process Analytical Technology: Spectroscopic Tools and Implementation Strategies for the Chemical and Pharmaceutical Industries*; Blackwell Pub: Ames, IA, USA, 2005.
7. Carloni, A.; Turner, A.P.F.; Flickinger, M.C. Bioprocess monitoring. In *Encyclopedia of Industrial Biotechnology*; John Wiley & Sons, Inc.: Hoboken, NJ, USA, 2009.
8. Potvin, G.; Ahmad, A.; Zhang, Z. Bioprocess engineering aspects of heterologous protein production in *Pichia pastoris*: A review. *Biochem. Eng. J.* **2012**, *64*, 91–105.
9. Kiviharju, K.; Salonen, K.; Moilanen, U.; Eerikäinen, T. Biomass measurement online: The performance of *in situ* measurements and software sensors. *J. Ind. Microbiol. Biotechnol.* **2008**, *35*, 657–665.
10. Davey, C.L.; Davey, H.M.; Kell, D.B. On the dielectric properties of cell suspensions at high volume fractions. *J. Electroanal. Chem.* **1992**, *343*, 319–340.
11. Downey, B.; Graham, L. The Use of Dielectric Scanning to Probe for Cellular Biomass, Viability, and Morphology in Laboratory, Pilot, and Industrial Bioreactors. Available online: <http://www.bendresearch.com/content/the-use-of-dielectric-scanning-to-probe-for-cellular-biomass-viability-and-morphology-in-lab> (accessed on 1 May 2015).
12. Markx, G.H.; Davey, C.L. The dielectric properties of biological cells at radiofrequencies: Applications in biotechnology. *Enzym. Microb. Technol.* **1999**, *25*, 161–171.
13. Carvell, J.P.; Dowd, J.E. On-line Measurements and Control of Viable Cell Density in Cell Culture Manufacturing Processes using Radio-frequency Impedance. *Cytotechnology* **2006**, *50*, 35–48.
14. Davey, C. *The Biomass Monitor Source Book*; Aber Instruments Ltd.: Aberystwyth, UK, 1993.
15. Noll, T.; Biselli, M. Dielectric spectroscopy in the cultivation of suspended and immobilized hybridoma cells. *J. Biotechnol.* **1998**, *63*, 187–198.
16. Cannizzaro, C.; Gügerli, R.; Marison, I.; von Stockar, U. On-line biomass monitoring of CHO perfusion culture with scanning dielectric spectroscopy. *Biotechnol. Bioeng.* **2003**, *84*, 597–610.
17. Opel, C.F.; Li, J.; Amanullah, A. Quantitative modeling of viable cell density, cell size, intracellular conductivity, and membrane capacitance in batch and fed-batch CHO processes using dielectric spectroscopy. *Biotechnol. Prog.* **2010**, *26*, 1187–1199.
18. Davey, C.L.; Davey, H.M.; Kell, D.B.; Todd, R.W. Introduction to the dielectric estimation of cellular biomass in real time, with special emphasis on measurements at high volume fractions. *Anal. Chim. Acta* **1993**, *279*, 155–161.
19. Párta, L.; Zalai, D.; Borbély, S.; Putics, Á. Application of dielectric spectroscopy for monitoring high cell density in monoclonal antibody producing CHO cell cultivations. *Bioprocess Biosyst. Eng.* **2014**, *37*, 311–323.

20. Justice, C.; Brix, A.; Freimark, D.; Kraume, M.; Pfromm, P.; Eichenmueller, B.; Czermak, P. Process control in cell culture technology using dielectric spectroscopy. *Biotechnol. Adv.* **2011**, *29*, 391–401.
21. Ducommun, P.; Kadouri, A.; von Stockar, U.; Marison, I.W. On-line determination of animal cell concentration in two industrial high-density culture processes by dielectric spectroscopy. *Biotechnol. Bioeng.* **2002**, *77*, 316–323.
22. El Wajgali, A.; Esteban, G.; Fournier, F.; Pinton, H.; Marc, A. Impact of microcarrier coverage on using permittivity for on-line monitoring high adherent Vero cell densities in perfusion bioreactors. *Biochem. Eng. J.* **2013**, *70*, 173–179.
23. Guan, Y.; Evans, P.M.; Kemp, R.B. Specific heat flow rate: An on-line monitor and potential control variable of specific metabolic rate in animal cell culture that combines microcalorimetry with dielectric spectroscopy. *Biotechnol. Bioeng.* **1998**, *58*, 464–477.
24. Von Stockar, U.; Maskow, T.; Liu, J.; Marison, I.W.; Patiño, R. Thermodynamics of microbial growth and metabolism: An analysis of the current situation. *J. Biotechnol.* **2006**, *121*, 517–533.
25. Doran, P.M. 5—Energy Balances. In *Bioprocess Engineering Principles*; Doran, P.M., Ed.; Academic Press: London, UK, 1995; pp. 86–109.
26. Marison, I.; Liu, J.-S.; Ampuero, S.; Von Stockar, U.; Schenker, B. Biological reaction calorimetry: Development of high sensitivity bio-calorimeters. *Thermochim. Acta* **1998**, *309*, 157–173.
27. Guan, Y.H.; Kemp, R.B. On-line heat flux measurements improve the culture medium for the growth and productivity of genetically engineered CHO cells. *Cytotechnology* **1999**, *30*, 107–120.
28. Kemp, R.B. “Fire burn and cauldron bubble” (W. Shakespeare): What the calorimetric–respirometric (CR) ratio does for our understanding of cells? *Thermochim. Acta* **2000**, *355*, 115–124.
29. Türker, M. Development of biocalorimetry as a technique for process monitoring and control in technical scale fermentations. *Thermochim. Acta* **2004**, *419*, 73–81.
30. García-Payo, M.C.; Ampuero, S.; Liu, J.S.; Marison, I.W.; von Stockar, U. The development and characterization of a high resolution bio-reaction calorimeter for weakly exothermic cultures. *Thermochim. Acta* **2002**, *391*, 25–39.
31. Voisard, D.; Pugeaud, P.; Kumar, A.R.; Jenny, K.; Jayaraman, K.; Marison, I.W.; von Stockar, U. Development of a large-scale biocalorimeter to monitor and control bioprocesses. *Biotechnol. Bioeng.* **2002**, *80*, 125–138.
32. Nienow, A.W. Reactor Engineering in Large Scale Animal Cell Culture. *Cytotechnology* **2006**, *50*, 9–33.
33. Doran, P.M. 8—Heat Transfer. In *Bioprocess Engineering Principles*; Doran, P.M., Ed.; Academic Press: London, UK, 1995; pp. 164–189.
34. Biener, R.; Steinkämper, A.; Hofmann, J. Calorimetric control for high cell density cultivation of a recombinant *Escherichia coli* strain. *J. Biotechnol.* **2010**, *146*, 45–53.
35. Biener, R.; Steinkämper, A.; Horn, T. Calorimetric control of the specific growth rate during fed-batch cultures of *Saccharomyces cerevisiae*. *J. Biotechnol.* **2012**, *160*, 195–201.
36. Schuler, M.M.; Sivaprakasam, S.; Freeland, B.; Hama, A.; Hughes, K.-M.; Marison, I.W. Investigation of the potential of biocalorimetry as a process analytical technology (PAT) tool for monitoring and control of Crabtree-negative yeast cultures. *Appl. Microbiol. Biotechnol.* **2012**, *93*, 575–584.

37. Sivaprakasam, S.; Mahadevan, S.; Bhattacharya, M. Biocalorimetric and respirometric studies on metabolic activity of aerobically grown batch culture of *Pseudomonas aeruginosa*. *Biotechnol. Bioprocess Eng.* **2007**, *12*, 340–347.
38. Voisard, D.; Claivaz, C.; Menoud, L.; Marison, I.W.; von Stockar, U. Use of reaction calorimetry to monitor and control microbial cultures producing industrially relevant secondary metabolites. *Thermochim. Acta* **1998**, *309*, 87–96.
39. Liu, J.-S.; Marison, I.W.; von Stockar, U. Microbial growth by a net heat up-take: A calorimetric and thermodynamic study on acetotrophic methanogenesis by *Methanosarcina barkeri*. *Biotechnol. Bioeng.* **2001**, *75*, 170–180.
40. Maskow, T.; Paufler, S. What does calorimetry and thermodynamics of living cells tell us? *Methods* **2015**, *76*, 3–10.
41. Han, W.S.; Stillman, G.A.; Lu, M.; Lu, C.; McPherson, B.J.; Park, E. Evaluation of potential nonisothermal processes and heat transport during CO<sub>2</sub> sequestration. *J. Geophys. Res. Solid Earth* **2010**, *115*, B07209.
42. Byrne, K. High Density CHO Cell Cultures: Improved Productivity and Product Quality. Ph.D. Thesis, School of Biotechnology, Dublin City University, Dublin, Ireland, 2014.
43. Cruz, H.J.; Freitas, C.M.; Alves, P.M.; Moreira, J.L.; Carrondo, M.J.T. Effects of ammonia and lactate on growth, metabolism, and productivity of BHK cells. *Enzym. Microb. Technol.* **2000**, *27*, 43–52.
44. Lao, M.-S.; Toth, D. Effects of Ammonium and Lactate on Growth and Metabolism of a Recombinant Chinese Hamster Ovary Cell Culture. *Biotechnol. Prog.* **1997**, *13*, 688–691.
45. Marks, D.M. Equipment design considerations for large scale cell culture. *Cytotechnology* **2003**, *42*, 21–33.

© 2015 by the authors; licensee MDPI, Basel, Switzerland. This article is an open access article distributed under the terms and conditions of the Creative Commons Attribution license (<http://creativecommons.org/licenses/by/4.0/>).